Organic & Biomolecular Chemistry

Cite this: *Org. Biomol. Chem.*, 2011, **9**, 400

www.rsc.org/obc

PAPER

Anti-malarial, anti-algal, anti-tubercular, anti-bacterial, anti-photosynthetic, and anti-fouling activity of diterpene and diterpene isonitriles from the tropical marine sponge *Cymbastela hooperi*†

Anthony D. Wright,*[a] Adam McCluskey,[b] Mark J. Robertson,[b] Kylie A. MacGregor,[b] Christopher P. Gordon[b] and Jana Guenther[c]

Received 26th June 2010, Accepted 16th September 2010
DOI: 10.1039/c0ob00326c

In an investigation into their potential ecological role(s), a group of mainly diterpene isonitriles, nine in total, isolated from the tropical marine sponge *Cymbastela hooperi*, and the sesquiterpene axisonitrile-3, isolated from the tropical marine sponge *Acanthella kletra*, were evaluated in a series of bioassays including anti-fouling, anti-algal, anti-photosynthetic, anti-bacterial (Gram +ve and –ve), anti-fungal, and anti-tubercular. The results of these assays showed that all of the tested compounds, with the exception of diterpene **9**, were active in at least two of the applied test systems, with axisonitrile-3 (**10**) and diterpene isonitrile **1** being the two most active compounds overall, closely followed by diterpene isonitrile **3**. Based on the results of the photosynthetic study a molecular modelling investigation was undertaken with all of the compounds used in that study. The results showed a positive correlation between reduction in photosynthetic activity and the interaction of the modelled compounds with a potential enzyme active site.

Introduction

Nature provides an unparalleled access to unique chemical scaffolds with novel modes of action against a myriad of disease targets. Marine natural products and their derivatives account for approximately 60% of the currently marketed pharmaceuticals, it is thus no surprise that exploration continues.[1–3] There is little doubt that medicinal chemistry in the 21st century will continue to rely on the natural product researchers to identify new biologically active scaffolds and it is imperative that the interaction between medicinal and natural products researchers and biology continues to flourish.

Often in the natural products arena the most difficult choices are in which disease to target and which marine organism to explore. Our team over the past decade or two has had an ongoing interest in the sponge *Cymbastela hooperi* van Soest, Desqueyroux–Faúndez, Wright, König (*C. hooperi*),[4] collected from the Kelso reef, Great Barrier Reef, Australia. *C. hooperi* has attracted considerable attention and is of interest not only taxonomically[4,5] but also chemically and biologically.[6–10] *C. hooperi* has proven to be a rich source of novel metabolites with a wide range of biological activities, and of particular note is the anti-malarial activity of a series of diterpenes and isonitrile-containing diterpenes (Fig. 1).

Malaria, the disease caused by the parasite *Plasmodium spp.*, still contributes significantly to human mortality, especially in developing countries. Poverty and lack of proper medical care intensify the strong impact of this disease. Every year over one million people die because of an infection by this protozoan parasite.[11,12] This situation is complicated by *Plasmodium's* intricate life cycle with host and development stage changes and our limited knowledge about these processes. *Plasmodium's* life cycle involves two types of hosts; cold (*Anopheles gambiae*) and warm (*e.g.* human). There are two human stages; liver and human blood (ring, trophozoic and schizont). Many researchers are currently examining anti-malarial vaccines and drugs. However, there remains a lack of efficient vaccinations, and *Plasmodium spp.* easily evolve to become resistant to intensively used anti-malarial drugs such as chloroquine and sulfadoxine.[13] Therefore, the development of new and inexpensive anti-malarial medicines is an important goal.

It was the isonitrile-containing diterpenes typified by **1–5** that enabled the anti-malarial activity mechanism of action of these,[7,14] and other isonitriles found in the marine environment, to be elucidated.[15] We have shown that isonitriles collected from *C. hooperi*, *e.g.* diisocyanoadociane (**4**), as well as axisonitrile-3 (**10**), both of which have potent anti-malarial activity, interact with heme by forming a coordination complex with the heme iron. Evidence amassed thus far indicates that the isonitrile moiety is crucial for activity, being able to form a coordinate bond with the iron of heme and, in doing so, probably interfering with its

[a]*College of Pharmacy, University of Hawaii at Hilo, Hilo, 96720, Hawaii, USA. E-mail: adwright@hawaii.edu; Fax: +1 808 933 2974; Tel: +1 808 933 2866*

[b]*Chemistry, University of Newcastle, Callaghan, NSW, 2308, Australia. E-mail: Adam.McCluskey@newcastle.edu.au; Fax: +61 249 215472; Tel: +61 249 216486*

[c]*Centre for Research-based Innovation in Aquaculture Technology, SINTEF Fisheries and Aquaculture, 7465, Trondheim, Norway*

† Electronic supplementary information (ESI) available: Supplementary information. See DOI: 10.1039/c0ob00326c

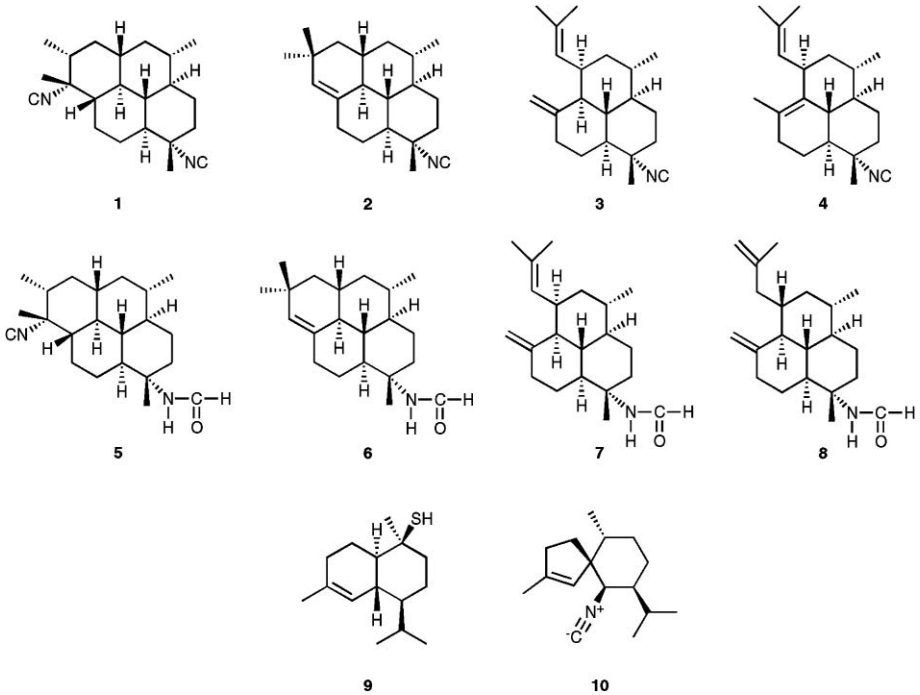

Fig. 1 Chemical structures of diterpene isonitriles **1–5** and diterpenes **6–9** isolated from *C. hooperi* and axisonitrile-3 (**10**) isolated from *Acanthella kletra*.

conversion to hemozoin. This probable mode of anti-malarial activity is likely for other anti-malarials, but to date is not proven. This mode of action and the excellent level of anti-malarial activity observed for many of these compounds has led to a number of synthetic approaches being developed based on the natural products findings, and has clearly shown the potential of these compounds as important lead structures in the search for new anti-malarial agents.[16]

Thus far, the biological activity assessment of this extensive and fascinating group of compounds, produced by a single animal, has been restricted to activities that may or may not have anything to do with their potential ecological function. This is a fairly typical approach in this type of biodiscovery research as amounts of isolates are often limited and normally exhausted by the end of a targeted round or two of bioassays. In this case however the animal tissue did yield sufficient amounts of compounds to enable further bioassays to be undertaken. It is known that nudibranchs do sequester sponge derived isonitriles into their skin,[17] and it has been proposed that these compounds in some way behave as a feeding deterrent and so protect the nudibranchs from predation, hence one role of this class of compound is fairly well established. Other roles, for example as anti-bacterial[18] and anti-fungal[19] agents, may be implied from certain studies but have not been explicitly demonstrated.

Results and discussion

In a continuation of our earlier exploration efforts into the potential ecological role(s) of a selected group of mainly diterpene isonitriles, herein we report our findings on the biological activity of nine diterpenes and diterpene isonitriles (**1–9**) derived from *C. hooperi* and axisonitrile-3 (**10**) isolated from the tropical marine sponge *Acanthella kletra*. Our initial screening focused on the anti-malarial properties of these compounds and the screening outcomes are given in Table 1.

Table 1 Biological activities of diterpene isonitriles **1–5** and diterpenes **6–9** from *C. hooperi* and axisonitrile-3 (**10**) against three *Plasmodium falciparum* malaria strains and determination of their cytotoxicity against the KB cell line

Compound	FCR3F85[a] Anti-malarial	D6[a]	W2[a]	KB cells[a] Cytotoxicity
1	—[b]	0.0047	0.0043	4.7
2	—	0.0741	0.0238	14.5
3	—	0.0141	0.0093	3.2
4	—	0.0585	0.0256	15.2
5	0.200	0.800	0.700	>20
6	>100	—	—	—
7	0.063	—	—	—
8	>90	—	—	—
9	—	3.600	2.900	>20
10	—	0.142	0.165	>20

[a] Values are IC_{50}s μg mL^{-1}; [b] "—" indicates a substance was not tested.

We used the FCR3F85, D6 and W2 strains of *Plasmodium falciparum*, one of the most common and virulent forms of *Plasmodium* species, in our evaluations. In these anti-malarial studies all compounds were also assessed for their cytotoxicity (in KB cells) so as to enable a selectivity of action index (SI) to be calculated (defined here as SI = [GI_{50} KB]/[IC_{50} anti-malarial]). The limited amounts of material available prevented all three *P. falciparum* strains being examined in full. However from the data presented in Table 1 it is evident that the isonitriles **1–10** (Fig. 1) display a range of anti-malarial activity; the most potent being **1** and **3** with IC_{50}(D6) values of 0.0047 to 0.0141 μg mL^{-1} and IC_{50}(W2) values of 0.0043 to 0.0093 μg mL^{-1}. Of these compounds **1** is the most active, and it also displays the highest D6 and W2 selectivity values with SI_{D6} ~ 1000 and SI_{W2} ~1100. These values

Table 2 Anti-bacterial (*Escherichia coli*, *Vibrio harvey*, *Bacillus megaterium*) and anti-fungal (*Ustilago violacea*, *Eurotium repens*, *Mycotypha microspora*, *Fusarium oxysporum*) activities of **1–10**

Compound	*Escherichia coli*[d]	*Vibrio harveyi*[a]	*Bacillus megaterium*[d]	*Ustilago violacea*[d]	*Eurotium repens*[d]	*Mycotypha microspora*[d]	*Fusarium oxysporum*[d]
	Anti-bacterial (Gram –ve)		Anti-bacterial (Gram +ve)	Anti-fungal			
1	1	2.5	3	—[e]	3	4	NA[f]
2	NA	NA	1	—	1	6	NA
3	NA	NA	2	—	2	10	NA
4	NA	NA	2	—	3	12	NA
5	NA	—	2	3	5	5	2
6	NA	—	NA	1	NA	1	NA
7	NA	—	1	3	2	1	NA
8	NA	—	NA	1	1	NA	NA
9	NA	—	NA	—	NA	NA	NA
10	1	250	2	—	2	2	NA

[a] Values are IC_{50}s μg mL^{-1}; [b] Values are IC_{50}s ng mL^{-1}; [c] Test concentration was 0.2 mg mL^{-1}; [d] Test concentration was 50 μg $disk^{-1}$ and inhibition was measured in mm from edge of disk; [e] "—" indicates a substance was not tested in the particular assay; [f] NA indicates a substance was considered inactive in a particular assay.

compare very favourably against SI_{D6} ~ 200 and SI_{W2} ~ 600 for **2**; and SI_{D6} ~ 225 and SI_{W2} ~ 350 for **3**. Against the FCR3F85 strain, both **5** and **7** are poorly active with IC_{50}s(FCR3F85) of 0.2 and 0.063 μg mL^{-1}, respectively. A similar trend is evident for **5** against D6 and W2 *P. falciparum* strains with IC_{50} values of 0.800 and 0.700 μg mL^{-1}, respectively. Notwithstanding this, **5** is the only analogue to display selectivity towards the FCR3F85 *P. falciparum* strain.

Towards the two Gram –ve bacteria, *Escherichia coli* and its marine equivalent *Vibrio harveyi*, only **1** and **10** were active (Table 2). Significantly, **1** was one hundred-fold more active towards *Vibrio harveyi* than was **10**. It is not common to find natural products that are active towards Gram –ve bacteria, even those that are known to be highly toxic. Why **1** and **10** are active towards these bacteria is unclear. The fact that they both are and that **1** is so much more active than **10** towards the marine derived *Vibrio harveyi* is clearly of some significance. However the lack of structure activity data amongst the other analogues prevents any logical conclusion being drawn or hypothesis developed. Towards the Gram +ve bacteria *Bacillus megaterium*, compounds **1–5**, **7** and **10** showed positive growth inhibition effects at the 50 μg $disk^{-1}$ level, with **1** having the most pronounced effect.

All compounds, with the exception of **9**, demonstrated anti-fungal activity towards one or more of the fungal strains employed. The most general anti-fungal compound was **5**, the only compound found to significantly inhibit the growth of all fungal species employed here. Not surprisingly, due to their structural similarities, both **3** and **4** were the next most active compounds in these assays.

We next turned our attention to examination of the anti-algal, anti-photosynthetic and anti-tubercular properties of isonitriles and diterpenes **1–10**, and these data are shown in Table 3.

Of the five compounds tested in the anti-tubercular assay, **1**, **3**, **4**, **9** and **10**, all, with the exception of **9**, the thiol, showed moderate activity with axisonitrile-3 (**10**) being the most active. This pattern of activity was very similar to that seen in some of the anti-bacterial and anti-fungal assays, but interestingly not in the anti-algal assay. What this means in terms of anti-tubercular activity is not clear, but it is certainly worthy of note that whilst

Table 3 Anti-algal (*Chlorella fusca*), anti-photosynthetic and anti-tubercular (*Mycobacterium tuberculosis*) activities of isonitriles **1–9** from *C. hooperi* and axisonitrile-3 (**10**)

Compound	*Chlorella fusca*[a]	*Photosynthesis reduction* (%)[b]	*Mycobacterium tuberculosis*[c]
	Anti-algal	Anti-photosynthesis	Anti-tubercular
1	2	36.9	8
2	3	0	—[d]
3	3	45.4	8
4	3	68.8	8
5	NA[e]	—	—
6	NA	—	—
7	NA	—	—
8	NA	—	—
9	4	—	>128
10	NA	0	2

[a] Test concentration was 50 μg $disk^{-1}$ and inhibition was measured in mm from edge of disk; [b] Test concentration was 0.2 mg mL^{-1}; [c] Values are IC_{50}s μg mL^{-1}; [d] NA indicates that the compound was not active in this assay; [e] "—" indicates a substance was not tested in the particular assay.

all of these compounds are active in a variety of anti-microbial assays, the mechanism of this action, although unknown, seems not to relate to general toxicity.

At the 50 μg $disk^{-1}$ level, **1–4** and **9** all inhibit the growth of the freshwater algae *Chlorella fusca* to a similar degree. This anti-algal assay examined the ability of **1–10** to inhibit the growth of *Chlorella fusca* to see if these compounds played any ecological role. It is known that tissue of this animal contains relatively high concentrations of photosynthetic organisms, which we thought may be responsible for the observed anti-algal and possibly anti-malarial activity. Whilst there are many possible mechanisms of action that would account for our observed anti-algal activity, *e.g.* cytotoxicity (it was known that **1–4** were mildly cytotoxic),[7] we felt that, given the levels of photosynthetic organisms, that the inhibition of photosynthesis may be at least in part responsible for the inhibition of algal growth.

Due to issues associated with compound availability, the anti-photosynthetic activity of only **1–4** and **10** were assessed. Although

10 was found to be generally inactive in the anti-algal assay, it was considered a possibility that this compound may in some way affect photosynthesis as it possesses key pharmacophoric moieties and other biological activities in common with **1–4**, and was thus included in the assay. Clearly, **1**, **3** and **4** do not completely inhibit the photosynthetic process with inhibition values of 36.9, 45.4 and 68.8% respectively, at a test concentration of 0.2 mg mL^{-1} (Table 3), suggesting they might have a regulatory role in controlling the growth of photosynthetic organisms within the sponge tissue rather than simply killing them. Compounds **2** and **10** had no observable effects in this assay.

On the basis of this, a molecular modelling study using the five compounds **1–4** and **10** was undertaken when it was realised that the porphyrin (heme)-containing proteins cytochromes b and f are involved both in photosystem II of the carbon fixation cycle of photosynthesis and in the promolgation of malaria, and hence the mode of action of **1**, **3** and **4** may be in some way be related to their anti-malarial activity, see Table 3.[7,14] The data presented in Table 3 suggests the mode of action of **2** involves something other than inhibition of photosynthesis and that axisonitrile-3 (**10**) has no effect on algal growth.

Initial docking simulations utilised the high resolution deoxy human haemoglobin crystal structure as a simple model of a heme-containing protein with obvious relevance to the anti-malarial activity of these compounds (PDB code 2DN2). The docking simulations were prepared and conducted using the AutoDock4 suite. With the exception of the addition of hydrogen atoms and removal of water molecules, the structure was subjected to docking simulations without alteration.

In order to establish potential inhibitor binding regions, analogue **1** was subjected to a blind docking simulation whereby the docking grid centred on chain-A encapsulating the entire domain. As illustrated in Fig. 2, the blind docking simulations afforded three major clusters, two located within the central cavity of the tetramer, and the third located within the cavity adjacent to heme. As the initial biological data indicated that the inhibitors directly interacted with heme, the "heme trench" posed a more valid binding region than the central tetramer cavity.

To investigate the potential inhibitor–enzyme binding interactions in greater detail, compounds **1–4**, and **10** were subjected to focused docking simulations in which the docking grid was centred on the heme trench. As illustrated in Fig. 3, the docked orientation of analogue **1** indicated that the predominant binding interactions were hydrophobic with the inhibitor in close proximity to Gly68, Ala69, and Leu64. Additionally, the C1 isonitrile moiety was flanked by Thr67. The other isonitrile moiety was in close proximity to Arg65 and Arg72, which partially offsets the negative charge, and also in close proximity to one of the heme carboxylates, which twists slightly to minimise the unfavourable isonitrile–carboxylate interaction. The degree of movement of these residues is limited by the confines of the binding site.

With the exception of the C1 isonitrile–Thr67 binding interaction, the docked orientation of compound **2** closely resembled that obtained for compound **1**, whilst the docked orientation of the other inactive derivative, compound **10**, displayed minimal binding interactions (ESI†). Most notably, the isonitrile moiety of compound **10** formed no significant interactions.

Thus, the initial docked conformations suggest that a three point anchor is required for activity, whereby the isonitriles form

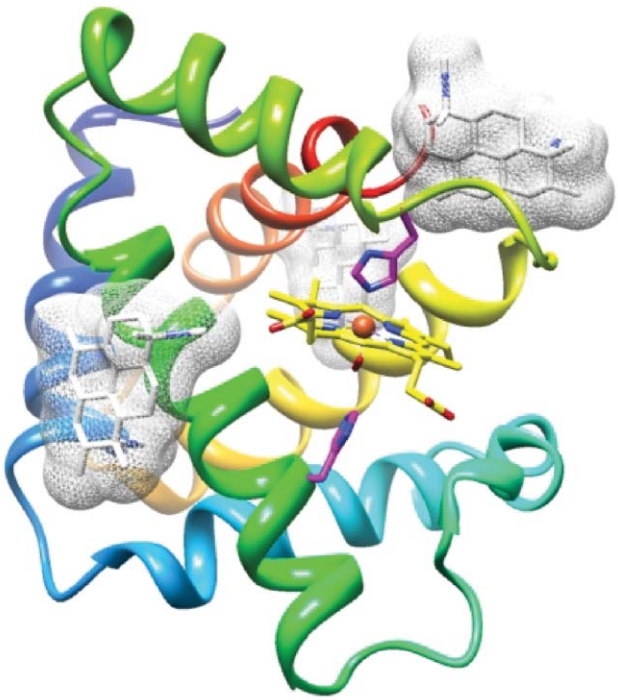

Fig. 2 Blind docking study of **1–4** and **10** and human haemoglobin (PDB code 2DN2). The lowest energy structures from the three major clusters are shown. The heme molecule is represented as sticks coloured yellow and by heteroatom type whilst the docked structures are stick representation coloured by atom with a van der Waals grid superimposed. For clarity only compound **1** is shown.

interactions with a heme carboxylate and Thr67 respectively, whilst the hydrophobic body occupies the heme trench. The docked orientations of **3** and **4** (ESI†) again closely resembled those obtained for **1** with the hydrophobic body occupying the heme trench whilst the isonitrile moieties flanked one of the heme carboxylates. Additionally, the sp^2 carbons of **3** and **4** adopted an orientation whereby they targeted the region flanked by Thr67 and Asn71, indicating the potential role of dipole–induced dipole interaction. However, as is always the case with models of this nature, the actual mode of interaction can only be determined either by co-crystallisation or *via* synthetic studies.

In efforts to further explore the binding mode of these isonitriles with heme containing proteins we also explored the blind docking of **1–4** and **10** with the heme containing plant cytochrome CYP74A (PDB code 3DAM) (Fig. 4).

Overall the primary compound clusters observed with analogues **1–4** and the plant cytochrome CYP74A resemble those found with human haemoglobin. We again note the presence of a central cavity binding pocket and a surface located "heme trench". With both orientations similar interactions are evident, with both interactions with the heme carboxylate and the hydrophobic nature of the pockets giving rise to the observed affinity for these sites. As with the human haemoglobin we believe that our data supports the "heme trench" as the more logical binding pocket.

The importance of an extended hydrophobic scaffold was further indicated with an additional docking simulation utilising a crystal structure of Gram –ve bacterial heme oxygenase (PDB code 1J77) and compound **4** (Fig. 5A). As with the haemoglobin

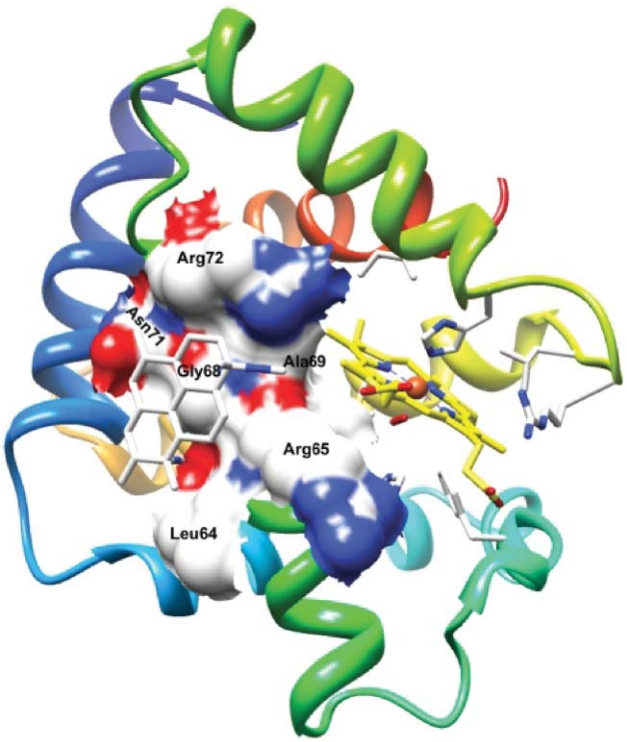

Fig. 3 Docked orientation of compound **1** and human haemoglobin (PDB code 2DN2). Compound **1** is represented as sticks and coloured by atom; the heme molecule is represented as sticks coloured yellow and by heteroatom type. Major amino acids lining the "heme trench" are annotated. For clarity only compound **1** is shown and hydrogen atoms are omitted. The partial solid surface represents the surface hydrophobicity.

and cytochrome simulations, the major docked cluster resided within a hydrophobic trench adjacent to the heme, however, in contrast to the haemoglobin simulations, isonitrile **4** sits above the heme. Nevertheless, the docking simulations indicate that the molecule's binding is to a conserved hydrophobic trench adjacent to the heme molecule. The sp^2 carbons of **4** adopt a conformation that facilitates interaction with Ala122 and Phe123, indicating that hydrophobic and π–π interactions may play a key role in stabilising the bioactive orientation.

As illustrated in Fig. 3–5, both the haemoglobin and the Gram –ve bacterial heme oxygenase docking simulations suggest **1–4** bind within an extended hydrophobic trench adjacent to the heme. The docking simulations indicate that binding affinities could be improved with the addition of an extended hydrophobic, possibly conjugated, moiety. Further, a conserved feature of the heme binding trench is a positively charged residue (Arg72 in haemoglobin, Lys131 in cytochrome CYP74A and Arg154 in bacterial heme oxygenase) toward the centre of the trench. The possible importance of this feature could be appraised with the addition of an electronegative moiety either within, or attached to the central inhibitor body, and may improve activity. On analysis of the predicted binding energies and pK_i values we note that there is good agreement with trends observed, with those analogues displaying good binding energies returning the best predicted pK_i values, which in turn broadly correlate with the observed inhibition of photosynthesis values (Table 4).

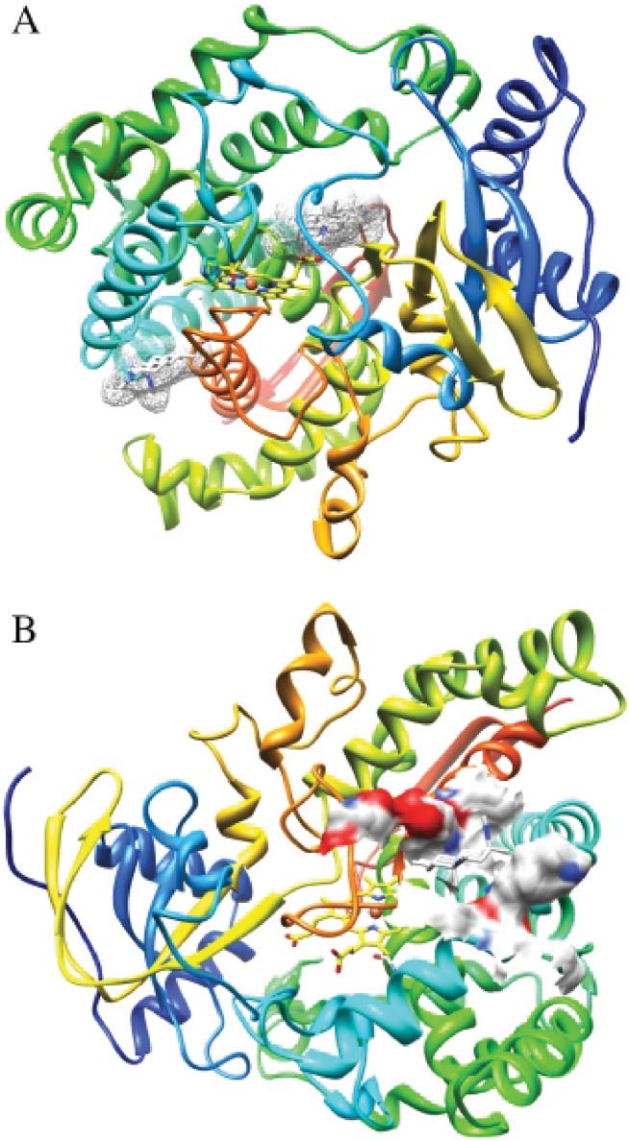

Fig. 4 (A) Docked orientations of **1–4** and **10** afforded from the heme containing plant cytochrome CYP74A (PDB code 3DAM). All compounds are shown in stick representation and coloured by atom. The heme molecule is represented as sticks coloured yellow and by heteroatom. For clarity only compound **1** is shown and hydrogen atoms are omitted. (B) Partial electrostatic surface shown with **1** binding predominately in the hydrophobic region with the isonitrile moieties stabilised by the local charged environment.

Table 4 The percent inhibition, calculated binding energies, and predicted binding constants of compound **1–4**, and **10**

Compound	Inhibition of Photosynthesis (%)	Binding Energy/ Kcal mol^{-1}	pK_i/μM
1	36.9	−6.9	14.08
2	0	−6.33	22.80
3	45.5	−6.62	8.69
4	68.8	−7.25	4.86
10	0	−5.15	168.73

Of the tested compounds (**1–4** and **10**), only compounds **1** and **10** were effective in deterring the settlement of an ecologically

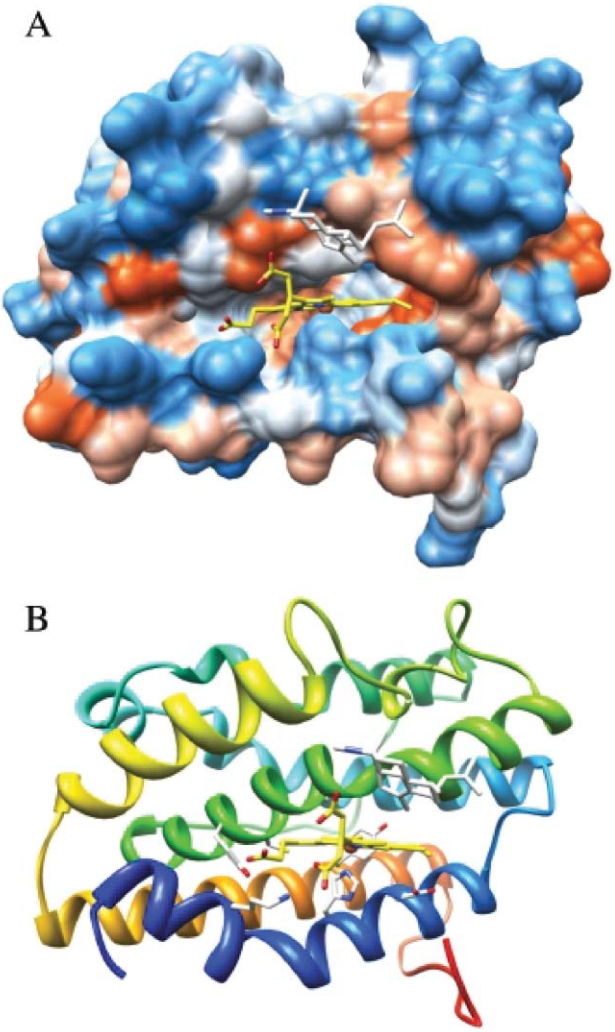

Fig. 5 (A) Docked orientations of compound **4** (stick representation, coloured by atom) afforded from the Gram –ve bacterial heme oxygenase simulations (PDB code 1J77). The heme molecule is represented as sticks coloured yellow and by heteroatom. (B) Docked orientation of compound **4** (stick representation, coloured by atom) afforded from the haemoglobin docking simulation. For simplicity hydrogen atoms are omitted. The solid surface represents the solvent accessible surface with a probe radius of 1.4 Å.

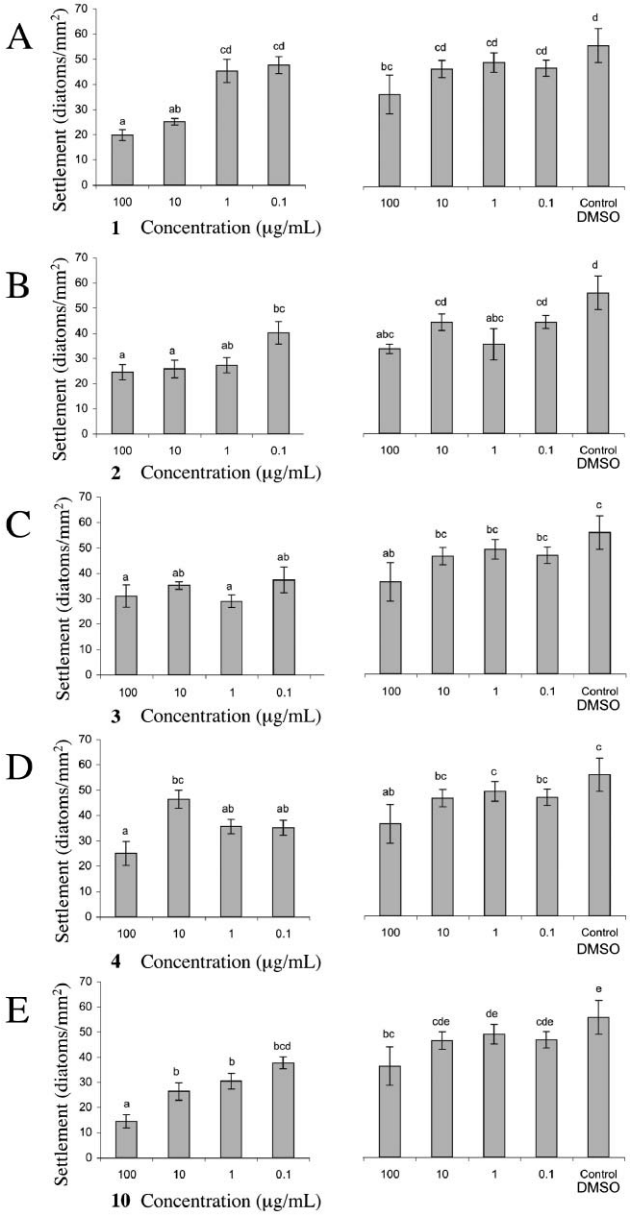

Fig. 6 Effects of analogues (A) **1**; (B) **2**; (C) **3**; (D) **4**; and (E) **10** on the settlement of the diatom *Nitzschia closterium* (diatoms mm^{-2}). Means ± SE are shown (n = 5 fields of view in each of 5 dishes). Different letters indicate significant differences (Tukey's HSD multiple comparison test, $p < 0.05$).

relevant fouling species (Fig. 6). Concentrations of 100 and 10 μg mL^{-1} of **1** and 100 μg mL^{-1} of **10** significantly reduced the settlement of the diatom *Nitzschia closterium* (Fig. 6A, E). The remaining compounds, **2–4**, did not have a statistically significant effect.

A range of studies have isolated compounds from sponges and demonstrated their anti-fouling activity.[20,21] While the results of these settlement assays are useful to determine the presence of potential anti-fouling compounds in the tissues of the sponges, further experiments are necessary to unequivocally determine an anti-fouling role of **1** and **10**. By identifying and quantifying surface-associated compounds and testing them at ecologically relevant concentrations against the settlement of fouling organisms, an anti-fouling role of compounds can be elucidated.[22,23] Regarding surface-associated compounds of sponges, only triterpene glycosides of the sponges *Erylus formosus* and *Ectyoplasia ferox* have been found to deter fouling organisms at biologically effective concentrations.[24] While this may be true for compounds reported to date, there is nothing reported that suggests compounds found in higher concentrations, *i.e.* those concentrations found for **1** and **10**, cannot also be behaving as natural anti-foulants.

Conclusions

The mainly diterpene isonitriles (**1–10**) isolated from *Cymbastela hooperi* and *Acanthella kletra* display a broad spectrum, and at times surprising, range of biological activities: anti-malarial, anti-algal, anti-tubercular, anti-bacterial, anti-photosynthetic and anti-fouling. With the exception of **9**, all analogues were active in

at least two of the applied test systems, with axisonitrile-3 (**10**) and **1** being the two most active compounds overall, closely followed by **3**. Isonitrile **1** displays the most promising anti-malarial activity both in terms of potency, analogues with IC_{50}(D6) of 0.0047 μg mL^{-1} and IC_{50}(W2) of 0.0043 μg $mL^{-1}$and selectivity with SI_{D6} ~ 1000 and SI_{W2} ~1100. This may form the basis of a new series of synthetic studies developing the medicinal chemistry of a novel series of anti-malarial compounds. In the anti-tubercular assay with **1**, **3**, **4**, **9** and **10**, all, with the exception of **9**, the thiol, showed moderate activity with axisonitrile-3 (**10**) being the most active. Due to issues associated with compound availability, the anti-photosynthetic activity of only compounds **1–4** and **10** was assessed. Although **10** was found to be generally inactive in the anti-algal assay it was considered a possibility that this compound may in some way affect photosynthesis, as it possesses key pharmacophoric moieties and other biological activities in common with **1–4**, and was thus included in the assay. Clearly, **1**, **3** and **4** do not completely inhibit the photosynthetic process with inhibition values of 36.9, 45.4 and 68.8% respectively at a test concentration of 0.2 mg mL (Table 3), suggesting they might have a regulatory role in controlling the growth of photosynthetic organisms within the sponge tissue rather than simply killing them. Compounds **2** and **10** had no observable effects in this assay. Our molecular modelling analyses suggest that these analogues bind in a "heme trench" and the degree of interaction correlates well with the observed anti-photosynthetic and anti-malarial activity. Further validation of these findings is underway in our efforts towards the rational design of novel anti-malarial activity.

Arguably the most surprising finding of this study was the anti-bacterial activity of **1** and **10** (against *Escherichia coli* and its marine equivalent *Vibrio harveyi*) with **1** being one hundred fold more active towards *Vibrio harveyi* than **10**. It is not common to find natural products that are active towards Gram –ve bacteria, even those that are known to be highly toxic. Why **1** and **10** are active towards these bacteria remains unclear. The fact that they both are and that **1** is so much more active than **10** towards the marine derived *Vibrio harveyi* is clearly of some significance.

General Experimental Procedures

As previously published.[4,6]

Tested Compounds

All tested compounds were isolated from previous studies according to published methods.[6,7,14,25]

Anti-malarial Activity

All details as previously reported.[7,14,25]

Anti-algal Activity

Compounds tested were dissolved in methanol and 50 μL of each (50 μg $disk^{-1}$) was pipetted onto a sterile antibiotic filter disc and placed onto CP-medium (10 g L^{-1} yeast extract; 10 g L^{-1} D-(+)-glucose monohydrate; 12 g L^{-1} agar) where they were then sprayed with a water suspension of *Chlorella fusca*. Zones of algal growth inhibition were measured in mm from the edge of the disk.

Anti-photosynthetic Activity

The green alga *C. fusca* was cultivated for 2 days in CP liquid medium (10 g glucose, 10 g yeast extract, 15 g agar, 1 L H_2O, pH adjusted to 6.2 prior to autoclaving); 50 mL portions of culture were incubated in 100 mL Erlenmeyer flasks on a shaker with 120 U min^{-1} at 20 °C. Before any measurements were made, the concentration of algae was adjusted to 1.8×10^7 cells mL^{-1} with a carbonate buffer (15% 0.1 mol L^{-1} Na_2CO_3, 85% 0.1 mol L^{-1} $NaHCO_3$). To achieve this, a known amount of algal culture was centrifuged for 5 min at 600 g and then suspended in the appropriate amount of buffer. The production of oxygen was measured with a P. J. Kipp and Zonen–Vertrieb-GmbH (Weisenau, Germany) model YSI 5331 oxygen electrode. The zero point of the electrode was established using Na_2SO_3 (50 g L^{-1}); 100% oxygen saturation was calibrated using distilled air-saturated H_2O (250 mL of H_2O being aerated with compressed air for 1 h). The reaction chamber was then filled with 5 mL of the algal suspension in buffer and kept in the dark until the oxygen content declined to zero. Subsequently, the suspension was illuminated, causing an increase of oxygen due to photosynthetic activity of the alga. At a concentration of 50% O_2 a 100 μL test solution was added. As a control, the reaction of the alga toward the solvent MeOH was tested.

Anti-fouling Activity

To test the anti-fouling activity of compounds **1–4** and **10** against the diatom *Nitzschia closterium* (CS-5, CSIRO) in laboratory based settlement assays, solutions with compounds at concentrations of 100, 10, 1 and 0.1 μg mL^{-1} of 0.45 μm filtered sea water (FSW) were prepared. Initial concentrations of these compounds were 10 mg mL^{-1} DMSO, except for **2** with 5 mg mL^{-1} DMSO. Subsequently, 3 mL of each solution was added to clear polystyrene Petri dishes (Sarstedt, diameter: 3.5 cm, base surface area: 9 cm^2) ($n = 4$). Control dishes containing DMSO in FSW as well as FSW only were also prepared. The diatom *N. closterium* was cultured in f2 media and kept in a temperature and light controlled room (25 °C, 12 h light : 12 h dark, Sylvania Tri-phosphor fluorescent lamps, 5200 lumens). To run settlement assays with *N. closterium*, 100 μL of a 2.5×10^5 algal cells mL^{-1} solution of *N. closterium* was added to each dish. The dishes were kept in the same temperature and light controlled room for 4 h. Subsequently, Petri dishes were dip rinsed 3 times in 0.45 μm FSW to remove unattached diatoms. Attached diatoms were counted with a compound microscope at ×200 magnification in 5 fields of view per dish.

All statistical analyses were performed with SPSS version 14. To determine significant differences in the settlement of the diatom *N. closterium* between treatments, the results were analysed with a 2-factor nested analysis of variance (factors: (1) treatment – 4 different concentrations of the crude extract and controls, (2) dish nested in treatment – 5 replicate dishes for each treatment) followed by Tukey's HSD multiple comparison tests. The assumptions of homogeneity and normality of the data were checked with residuals *versus* predicted values plots and Q–Q plots of residuals, respectively. If assumptions of homogeneity and normality were not met, the data were square root transformed.[26,27]

Anti-bacterial Activity

Activity of compounds was tested in agar diffusion assays against the bacteria *Bacillus megaterium*, *Escherichia coli*. Tested

compounds were dissolved in methanol and 50 μL of each (50 μg disk^{-1}) was pipetted onto a sterile antibiotic filter disc and placed onto NB medium (7.8 g L^{-1} peptone from meat, Merck; 7.8 g L^{-1} peptone from casein, Merck; 2.8 g L^{-1} yeast extract, Oxoid; 5.6 g L^{-1} NaCl, D-(+)-glucose monohydrate, Merck; 12 g L^{-1} agar, IMA) where they were then sprayed with a water suspension of the test bacteria. Where present, zones of bacterial growth inhibition were measured in mm from the edge of the disk.

Anti-fungal Activity

The fungi *Microbotryum violaceum*, *Eurotium repens*, *Fusarium oxysporum*, *Mycotypha microsporum* were used to assess the anti-fungal activity of all compounds. For the assays, test compounds were dissolved in methanol and 50 μL of each (50 μg disk^{-1}) was pipetted onto a sterile antibiotic filter disc and placed onto MPY-medium (as for bacteria but with 12 g L^{-1} agar) where they were then sprayed with a water suspension of the appropriate fungus. Zones of growth inhibition were measured in mm from the edge of the disk.

Anti-tubercular Activity

All details as previously reported (TB).[28]

Molecular Modelling

Blind docking simulation was conducted using PDB X-ray structure 2DN2. The crystal structure was prepared for docking utilising the molecular visualisation software package DS Viewer Pro whereby hydrogen atoms were added and the water molecules removed. The ligand was constructed *de novo* again using DS Viewer Pro. The ligand was further prepared using the utilities implemented by autodock tools (ADT) where lone pairs were merged and charges were assigned using the Gasteiger–Marsilli formalism. The ligand rigid root, to which the rotatable groups are connected, was assigned automatically as were the active torsions. The enzyme was also further prepared using the utilities implemented by ADT, enzyme non-polar hydrogens were merged, Kollman united-atom partial charges were assigned, polar hydrogens were merged and solvation parameters were added. Again using ADT the enzyme was embedded in a grid centred at atomic coordinates 23.246, 18.436, 23.715 with dimensions of 60 × 60 × 60 points and a spacing of 0.75 Å between grid points. Electrostatic grid maps were generated for each atom type in the ligand using the auxiliary program AutoGrid4. The docked conformations were generated using the Lamarckian genetic algorithm. Global optimisation started with a population of 50 individuals and a maximum of 1.0× 106 energy evaluations. A maximum of 27000 generations were produced with a total of 200 docking runs (ga runs) performed. Remaining parameters were retained at AutoDock 4.0 defaults.

Analysis of docking simulations was conducted with ADT using cluster analysis. The RMSD tolerance was set to 2.0 Å. The conformation with the lowest energy within the most populated cluster was deemed the final docked conformation. Visualisation of docking simulations was performed using DS Viewer Pro. With the exception of hydrogen bonding, which was calculated up to 2.0 Å, ligand enzyme interactions were determined *via* manual inspection. Enzyme solid surfaces were represented as solvent assessable surfaces with a probe radius of 1.4 Å. With the exception of the grid centre, 10.35 12.683 17.899, grid dimensions, (60 × 60 × 60 points) and a spacing of between grid points (0.375 Å) the focused docking simulations were conducted as described for the initial blind simulation.

The gram-negative bacterial heme oxygenase (PDB code 1J77) docking simulations were conducted as described for the focused haemoglobin docking simulations with grid centre at 10.35 12.683 17.899, grid dimensions, (60 × 60 × 60 points) and a spacing between grid points of 0.375 Å.

Acknowledgements

We thank C. Dreikorn, TU-Braunschweig, Braunschweig, Germany, for undertaking the anti-fungal, anti-bacterial, anti-algal and anti-photosynthetic assays, and J. Doyle, Australian Institute for Marine Sciences, Townsville, Queensland, Australia for undertaking the anti-bacterial assay with *Vibrio harveyi*.

Notes and references

1 D. J. Newman, *J. Med. Chem.*, 2008, **51**, 2589–2599.
2 I. Ojima, *J. Med. Chem.*, 2008, **51**, 2587–2588.
3 J. Rosn, J. Gottfries, S. Muresan, A. Backlund and T. I. Oprea, *J. Med. Chem.*, 2009, **52**, 1953–1962.
4 R. W. M. Van Soest, R. Desqueyroux-Faúndez, A. D. Wright and G. M. König, *Bull. Inst. R. Sci. Nat. Belg.*, 1996, **66**(suppl.), 103–108.
5 G. M. König and A. D. Wright, *Mem. Qld. Mus.*, 1999, **44**, 281–288.
6 G. M. König and A. D. Wright, *J. Org. Chem.*, 1997, **62**, 3837–3840.
7 G. M. König, A. D. Wright and C. K. Angerhofer, *J. Org. Chem.*, 1996, **61**, 3259–3267.
8 A. Linden, G. M. König and A. D. Wright, *Acta Crystallogr., Sect. C: Cryst. Struct. Commun.*, 1996, **C52**, 2601–2607.
9 A. D. Wright, G. M. König, C. K. Angerhofer, P. Greenidge, A. Linden and R. Desqueyroux-Faúndez, *J. Nat. Prod.*, 1996, **59**, 710–716.
10 A. D. Wright, H. Wang, M. Gurrath, G. M. König, G. Kocak, G. Neumann, P. Loria, M. Foley and L. Tilley, *J. Med. Chem.*, 2001, **44**, 873–885.
11 G. G. Van Dooren and G. I. McFadden, *Nature*, 2007, **450**, 955–956.
12 D. A. Fidock, P. J. Rosenthal, S. L. Croft, R. Reto Brun and S. Nwaka, *Nat. Rev. Drug Discovery*, 2004, **3**, 509–520.
13 T. W. A. Kooij, C. J. Janse and A. P. Waters, *Nat. Rev. Microbiol.*, 2006, **4**, 344–57.
14 C. K. Angerhofer, J. Pezzuto, G. M. König, A. D. Wright and O. Sticher, *J. Nat. Prod.*, 1992, **55**, 1787–1789.
15 G. M. König, A. D. Wright, S. Draeger, H.-J. Aust and B. Schultz, *J. Nat. Prod.*, 1999, **62**, 155–157.
16 O. Schwarz, R. Brun, J. W. Bats and H.-G. Schmalza, *Tetrahedron Lett.*, 2002, **43**, 1009–1013.
17 S. W. Ayer and R. J. Andersen, *Tetrahedron Lett.*, 1982, **23**, 1039–1042.
18 K. Benkendorff, A. R. Davis and J. B. Bremner, *J. Invertebr. Pathol.*, 2001, **78**, 109–118.
19 L. Gunthorpe and A. M. Cameron, *Mar. Biol.*, 1987, **94**, 39–43.
20 V. P. L. Mol, T. V. Raveendran and P. S. Parameswaran, *Int. Biodeterior. Biodegrad.*, 2009, **63**, 67–72.
21 M. Stewart, C. Depree and K. J. Thompson, *Nat. Prod. Comm.*, 2009, **4**, 331–336.
22 S. A. Dworjanyn, R. de Nys and P. D. Steinberg, *Mar. Ecol.: Prog. Ser.*, 2006, **318**, 153–163.
23 G. M. Nylund, P. E. Gribben, R. de Nys, P. D. Steinberg and H. Pavia, *Mar. Ecol.: Prog. Ser.*, 2007, **329**, 73–84.
24 J. Kubanek, K. E. Whalen, S. Engel, S. R. Kelly, T. P. Henkel, W. Fenical and J. R. Pawlik, *Oecologia*, 2002, **131**, 125–136.
25 A. D. Wright and N. Lang-Unnasch, *J. Nat. Prod.*, 2009, **72**, 492–495.
26 A. J. Underwood, *Oceanogr. Mar. Biol. Ann. Rev.*, 1981, **19**, 513–605.
27 G. P. Quinn and M. J. Keough, 2002, *Experimental design and data analysis for biologists*, Cambridge University Press, Cambridge.
28 G. M. König, A. D. Wright and S. G. Franzblau, *Planta Med.*, 2000, **66**, 337–342.